Chapter 2 Open Pit

2.1 Introduction

This chapter reports on the Mary Kathleen uranium mine void. The open cut is largely in the same form as it existed when mining stopped in 1982, it therefore provides a unique opportunity for studying a final uranium mine void.

The main objectives of this work were to establish the surficial mineralogical and geochemical composition and radioactivity of the Mary Kathleen void, to establish the sources, nature and magnitude of contamination and radioactivity in the open pit, and to discuss the management of the void in the light of possible end-use options. Ore, waste, mineral efflorescence, soil, vegetation and pit water samples were collected (Figure 2.1). Detailed radiometric traverses followed pit benches, the main haul road and crossed the pit waste rock piles.

2.2 Physical characteristics

The open pit is roughly circular in shape. The pit has a maximum depth of 230 meters, measured from the highest part of the eastern face to the pit base. The pit benches are referred to as relative levels (RL) in meters relative to topographic height. Phase one mining saw the open pit base at RL1000. The lowest pit level at the completion of mining is RL888. Pit wall geometry has 8 m benches with 24 m faces angled at 10° from the vertical separated by benches 10 m wide. Wider catch-benches (15 m wide - RL936 and RL1000) were created to hold falling rock, particularly near the shear zone.

The main haul road (to RL888) is a spiral decline 15 m wide at a gradient of 1 in 10. The north access (to RL984 and RL1000), south access (to RL1000) and the main pit haul roads and hence the pit benches (RL888 to RL1112), are blocked off to vehicular and cattle access with barriers of benign waste rock. The four main access roads were ripped and seeded. One small waste rock pile, (approximately 50 cubic meters) remains in the open pit (RL944). The water within the open pit is currently at RL940. Extensive and colourful mineral efflorescences are well developed on the pit walls. Daily temperatures within the pit reach 50°C (October).

Figure 2.1 Open pit sample location map (1:5000).

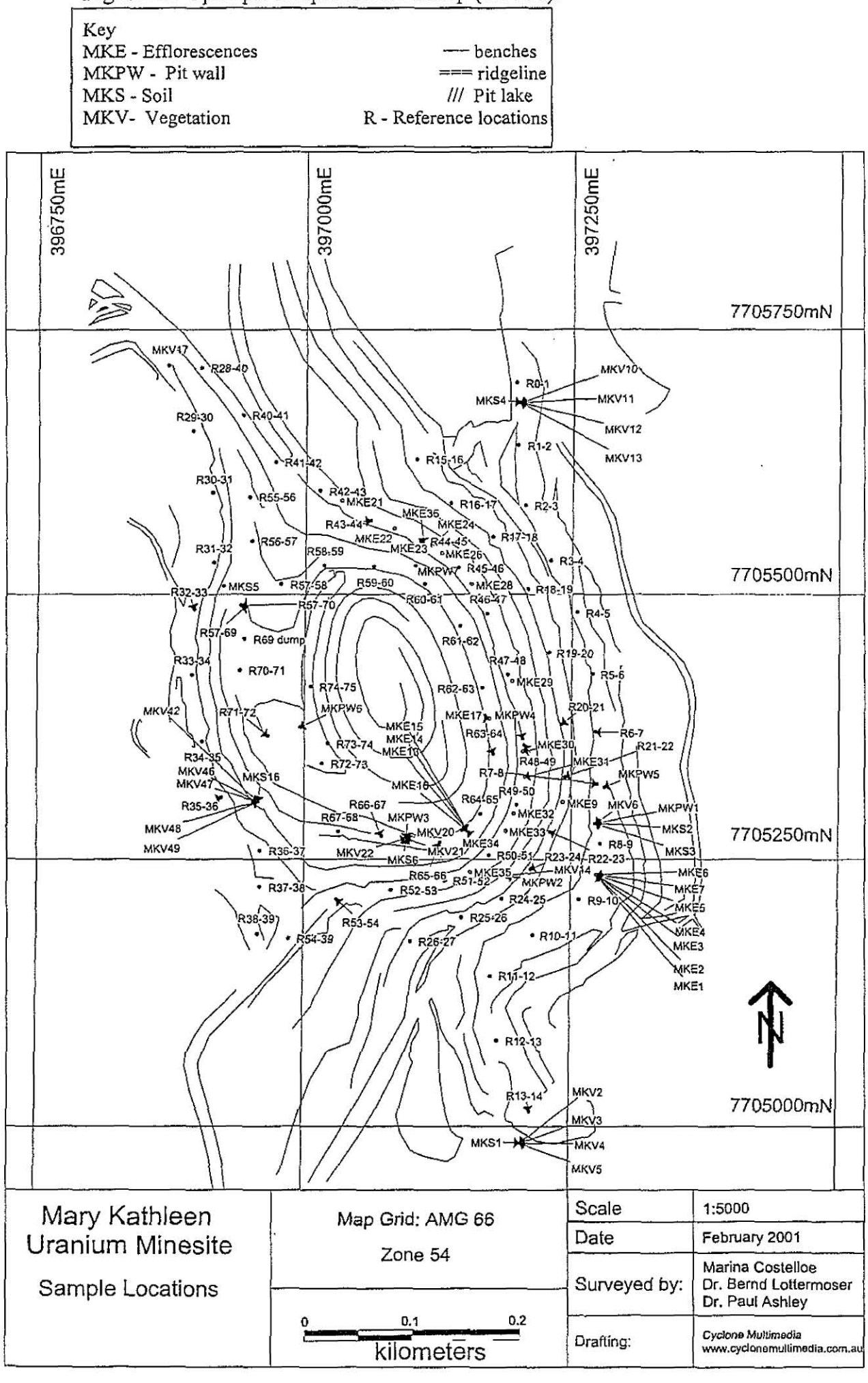

The exposed northern pit face exhibits large breccia fragments in a matrix of garnet and diopside. Mineralisation is distinguishable from gangue rock by its darker colour. Ore shoots on the north wall cut foliated metaconglomerate. The Mary Kathleen Shear zone on the southern pit face consists of a number of discrete zones of strongly sheared rock cutting the benches (Figure 2.2). The shear is strongly weathered at the surface and has a lack of mineral efflorescences. A spring and small wetland zone are present at level 944 near the Mary Kathleen Shear zone. The lowest pit face (west) and the entrance to the pit (north-west) have stable slopes. Small rockfalls are common and materials accumulate at the base of most benches. Calcite-rich veins cut the pit wall features except within the shear zone.

Figure 2.2. Photograph of the open pit east and south faces (Photographed 10-10-1999).

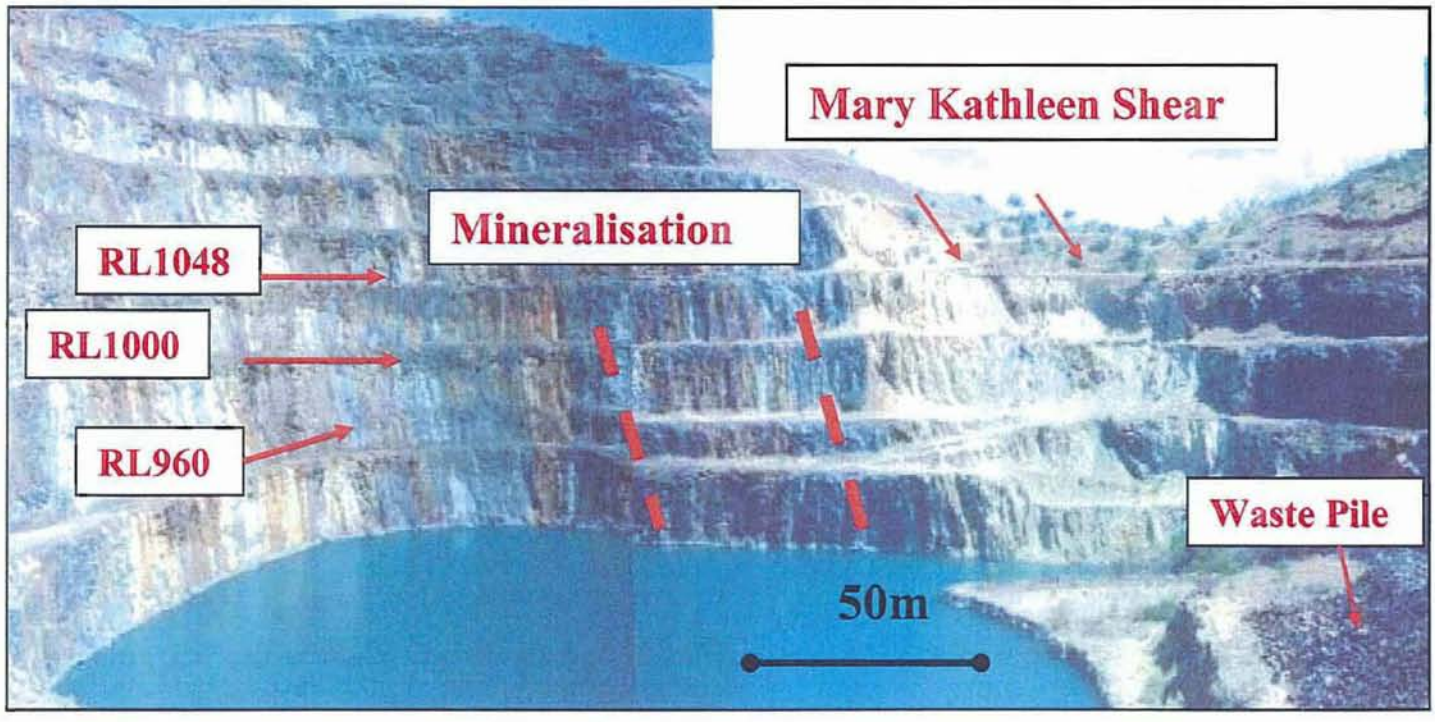

2.3 Pit wall samples

The Mary Kathleen ore is unique due to the elevated uranium concentrations and significant rare earth element (REE) contents. The ore consists of major garnet (andradite $Ca_3Fe^{2+}{}_2(SiO_4)_3$ - grossular $Ca_3Al_2(SiO_4)_3$) and clinopyroxene (diopside $CaMg(Si_2O_6)$), and accessory allanite ($(Ca,Ce,La)_2(Al,Fe)_3(SiO_4)_3(OH)$), chlorite ($(Mg,Fe)_5Al(AlSi_3)O_{10}(OH)_9$), calcite ($CaCO_3$), sericite ($K.Al_2(AlSi_3O_{10})(OH)_2$), epidote ($Ca_2(Al,Fe)_3(SiO_4)_3(OH)$), hornblende ($Ca_2Fe^{2+}{}_4Al_{0.75}Fe^{3+}{}_{0.25}(Si_7AlO_{22})(OH)_2$), prehnite ($Ca_2Al_2Si_3O_{10}(OH)$), scapolite ($Na_2Ca_2Al_3Si_9O_{24}Cl$) , plagioclase ($Na_{0.5}Ca_{0.5}Si_3AlO_8$), titanite ($CaTiO(SiO_4)$), stillwellite ($(Ce,La,Ca)BSiO_5$)), pyrrhotite ($Fe^{2+}{}_{0.95}S$), chalcopyrite ($CuFeS_2$), pyrite ($FeS_2$), marcasite ($FeS_2$), galena (PbS), sphalerite ((Zn,Fe)S), molybdenite (MoS_2), pentlandite ($(Fe,Ni)_9S_8$), bornite (Cu_5FeS_4) and linnaeite (Co_3S_4) and uraninite (UO_2) (McKay and Miezitis, 2001).

Rock chip samples and ore zone material were collected from pit wall benches (Appendix 9) and thin section descriptions are given below (Ashley unpub. data). Mineralisation occurs as semi-massive medium to coarse grained allanite-rich rock, with subordinate amounts of intergrown apatite ($Ca_5F(PO_4)_3$), and minor calcite. Late stage thin extensional calcite veins and pyrite as veinlets in allanite are noted. Medium to coarse grained in-equigranular garnet (Ca-rich), locally intergrown with patchy amounts of apatite also occur. Allanite and garnet are intergrown with scattered aggregates and disseminations of pyrrhotite and chalcopyrite, with pyrrhotite locally replaced by pyrite. Traces of uraninite are enclosed in garnet and allanite.

Average (n=7) pit wall samples (Table 2.1) contain high mean concentrations of Ca (17 wt%), Fe (11 wt%) and S (1 wt%) consistent with metamorphosed calc-silicate, mafic to intermediate igneous and sedimentary host rocks. Elevated mean levels of Cu (1973 ppm), Ce (6973 ppm), La (4742 ppm), and U (544 ppm) are also present, and are accounted for by abundant chalcopyrite, allanite, stillwellite and uraninite. Elevated Mo, Ni, P, and Y levels in ore material, far exceeds levels recognised in typical crustal abundance and also surrounding background material. As, Th and to a lesser extent Pb, are also commonly anomalous and exceed crustal abundance levels and background levels by more than ten times. It is assumed that most of the Cu, Ni, Ce, and La are held in primary ore minerals (e.g. chalcopyrite, allanite, pentlandite and stillwellite)

Table 2.1 Major (wt%) and trace element (ppm) geochemistry of pit wall samples.

	Ca	K	Fe	Mg	Na
Sample	%	%	%	%	%
MKPW1	7.7	1.1	17.4	0.7	1.1
MKPW2	17.9	0.4	9.0	1.5	0.7
MKPW3	18.4	0.3	9.5	1.6	0.5
MKPW4	19.1	0.2	10.3	0.9	0.3
MKPW5	20.6	0.1	11.7	1.1	0.3
MKPW6	21.6	0.0	10.6	0.4	0.1
MKPW7	16.0	0.8	8.5	1.0	0.9
Mean	17.3	0.4	11.0	1.0	0.6

	As	Ba	Ce	Cu	La	Mn	Mo	Ni	P	Pb	S	Sr	Th	U	V	Y	Zn
Sample	ppm	ppm	ppm	ppm	ppm	ppm	ppm	ppm	ppm	ppm	ppm	ppm	ppm	ppm	ppm	ppm	ppm
MKPW1	67	180	321	11600	180	1300	15	600	554	5	60710	23	13	18	118	29	22
MKPW2	66	52	3910	116	2820	2750	8	31	1780	83	1400	21	108	304	139	66	15
MKPW3	48	40	3010	168	2120	2890	7	36	1430	67	1140	10	88	277	93	53	15
MKPW4	185	27	14600	234	9490	2710	11	41	5360	222	2290	10	441	685	96	67	16
MKPW5	94	10	6130	1280	4860	2860	11	93	2950	86	10700	10	160	281	94	70	13
MKPW6	136	10	9530	113	6600	2970	10	17	4900	295	951	10	259	885	120	67	9
MKPW7	132	130	11310	302	7130	2330	11	43	4600	423	1970	22	152	1360	104	57	14
Mean	104	61	6973	1973	4743	2544	10	123	3082	169	11309	9	175	544	109	58	15

2.4 Mineral efflorescences

During mining and during care and maintenance between mining phases (1963-1975), there was no evidence of oxidation (Figure 2.3) on pit faces (Scott and Scott, 1985). In contrast, contemporary precipitation of yellow, orange, green and white mineral efflorescences on the pit walls is the main distinguishing physical feature of the open pit. Crystalline masses form under rock faces in crevices, fractures, at bench bases and as staining on rock faces (Figure 2.4). Pit wall efflorescences identified by XRD are listed in Table 2.2.

Figure 2.3. Open pit in the early 1960s (Mary Kathleen Museum).

Table 2.2. Mineral efflorescences identified from the open pit walls.

Sample ID	Mineral **Major phase** Minor phase	Chemical Formula (standard)
MKE1	**Melanterite**	$FeSO_4.7H_2O$
	Copiapite	$(Fe, Mg)Fe_4(SO_4)_6(OH)_2 . 20H_2O$
MKE2	**Melanterite**, Copapite	$FeSO_4.7H_2O$, $(Fe, Mg)Fe_4(SO_4)_6(OH)_2 . 20H_2O$
	Roemerite, Chalcanthite	$FeSO_4.Fe_2(SO_4)_3 \cdot 14(H_2O)$, $Cu(SO_4) \cdot 5(H_2O)$
MKE3	**Melanterite**	$FeSO_4.7H_2O$
	Roemerite,Chalcanthite	$FeSO_4.Fe_2(SO_4)_3 \cdot 14(H_2O)$, $Cu(SO_4) \cdot 5(H_2O)$
	Halotrichite, Copiapite	$Fe^{2+}Al_2(SO_4)_4 \cdot 22(H_2O)$, $(Fe, Mg)Fe_4(SO_4)_6(OH)_2 . 20H_2O$
MKE4	**Copiapite**	$(Fe, Mg)Fe_4(SO_4)_6(OH)_2 . 20H_2O$
	Melanterite, Halotrichite	$FeSO_4.7H_2O$, $Fe^{2+}Al_2(SO_4)_4 \cdot 22(H_2O)$
MKE7	**Copiapite**	$(Fe, Mg)Fe_4(SO_4)_6(OH)_2 . 20H_2O$
	Chalcanthite, Gypsum	$Cu(SO_4) \cdot 5(H_2O)$, $CaSO_4.2H_2O$
MKE8	**Copiapite**	$(Fe, Mg)Fe_4(SO_4)_6(OH)_2 . 20H_2O$
	Halotrichite, Melanterite	$Fe^{2+}Al_2(SO_4)_4 \cdot 22(H_2O)$, $FeSO_4.7H_2O$
MKE9	**Copiapite**	$(Fe, Mg)Fe_4(SO_4)_6(OH)_2 . 20H_2O$
	Melanterite	$FeSO_4.7H_2O$
MKE11	**Gypsum**	$CaSO_4.2H_2O$
	Copiapite	$(Fe, Mg)Fe_4(SO_4)_6(OH)_2 . 20H_2O$
MKE12	**Copiapite** (Mg and Fe)	$(Fe, Mg)Fe_4(SO_4)_6(OH)_2 . 20H_2O$
	Epsomite,Gypsum	$MgSO_4.7H_2O$, $CaSO_4.2H_2O$
MKE22	**Gypsum**	$CaSO_4.2H_2O$
MKE24	**Gypsum**	$CaSO_4.2H_2O$
	Melanterite,Copiapite	$FeSO_4.7H_2O$, $(Fe, Mg)Fe_4(SO_4)_6(OH)_2 . 20H_2O$
MKE25	**Gypsum**	$CaSO_4.2H_2O$
MKE26	**Gypsum**	$CaSO_4.2H_2O$
MKE28	**Gypsum**	$CaSO_4.2H_2O$
MKE29	**Gypsum,**	$CaSO_4.2H_2O$
	Epsomite,Copiapite	$MgSO_4.7H_2O$, $(Fe, Mg)Fe_4(SO_4)_6(OH)_2 . 20H_2O$
MKE30	**Gypsum**	$CaSO_4.2H_2O$
	Epsomite	$MgSO_4.7H_2O$
MKE31	**Gypsum**	$CaSO_4.2H_2O$
	Epsomite	$MgSO_4.7H_2O$
MKE32	**Gypsum**	$CaSO_4.2H_2O$

Small amounts of bright green, crushed hair-like crystals on mineralised rock (MKE13, MKE15, MKE17, MKE27) is tentatively identified as cuprosklodowskite ($Cu(UO_2)_2Si_2O_7 . 6H_2O$).

Based on colour, four efflorescence samples were submitted for geochemical analysis (Table 2.3).

Table 2.3. Major (wt%) and trace element (ppm) geochemistry of MKE3, MKE4, MKE8 and MKE31.

	Ca	Fe	K	Mg	Na	As	Ba	Ce	Cu	La	Mn	Ni	P	S	Th	U	Y	Zn
	%					ppm												
MKE3	Melanterite (roemerite, chalcanthite, halotrichite, copiapite)																	
green	0.1	17	<0.1	0.29	<0.1	<5	<1	121	534	75	454	948	19	114400	3	3	3	15
MKE4	Copiapite (melanterite, halotrichite)																	
Lt green	0.32	13	0.04	0.36	0.06	18	11	320	6900	214	858	1480	118	139310	19	17	18	18
MKE8	Copiapite (halotrichite, melanterite)																	
white	0.06	3	<0.1	1.88	0.02	24	<1	2010	6610	1400	3790	2360	91	142300	512	96	58	55
MKE31	Gypsum (epsomite)																	
orange	12.42	0	0.07	0.13	0.04	5	<1	788	238	456	51	31	21	96000	78	2	3	<5

MKE3 (Figure 2.4b) contains elevated levels of Fe (17 wt%) Cu (534 ppm) and S (114400 ppm) confirming XRD observations of melanterite, roemerite, copiapite and chalcanthite. MKE4 has high Fe (12.55 wt%), Cu (6900 ppm) and S (139310 ppm) reflecting copiapite, melanterite and halotrichite. The gypsum and epsomite rich sample (MKE31) contains high Ca (12 wt%), Mg (0.13 wt%) and S (96000 ppm).

MKE8 contains high Mg (1.88 wt%), Cu (6610 ppm), Mn (3790 ppm), Ni (2360 ppm), Ce (2010 ppm), La (1400 ppm) and U (96 ppm) and relatively low Fe (3 wt%). In MKE8 the geochemical technique (hot mixed acid digest and analysed by inductively coupled plasma optical emission and mass spectrometry techniques IC587 and MS587) only dissolved some of the sample material as indicated by the low iron content. However, the relatively high magnesium content suggests substitution of Fe by Mg in the crystal lattice of copiapite (i.e. Mg-copiapite). The detected trace elements Cu, Mn, Ni, Ce, La, Th and U may substitute for iron in these efflorescences and or they may be present in phases not detected by XRD.

Figure 2.4. Photographs of mineral efflorescences from the northern open pit wall

2.4b MKE field and SEM photographs

2.4c MKE33 field and SEM photographs (Photographs taken 10-10-1999)

Figure 2.4a. Northern open pit wall (note crusts of mineral efflorescences.)
Figure 2.4b. Field and SEM photographs of MKE3 Melanterite (Fe and Mn rich) occurs as the major phase with minor copiapite, roemerite, and halotrichite.
Figure 2.4c. Field photo and SEM photograph of MKE31 gypsum with minor epsomite.

2.5 Soil

2.5.1 Background soil

Background soil samples were taken approximately 1 to 5 km from the mine site (away from known mineralised areas and contamination sites). Background soil mineralogy is dominated by quartz, albite and microcline. Geochemical analysis (Table 2.4), indicates nutrient poor (mean P 757 ppm) soil with low metal, U and REE concentrations (Cu 60 ppm, Fe 4 wt%, Ce 108 ppm, La 53 ppm, U 6 ppm). Arsenic results were below detection limits (< 1 ppm).

Table 2.4. Major (wt%) and trace element (ppm) geochemistry of background soil.

Sample	Ca	Fe	K	Mg	Na	Ba	Ce	Cu	La	Mn	Ni	P	Pb	S	Sr	Th	U	V	Y	Zn
	%					ppm														
MKS13	4.6	9.3	1.1	3.2	1.9	168	42.6	143	18	1400	48	1030	6	84	104	5	1	350	43	74
MKS14	1.3	4.2	3.4	0.6	1.1	717	110	35	51	472	10	1140	15	41	94	36	8	78	62	32
MKS15	1.1	2.7	2.0	0.4	2.3	209	155	17	71	311	11	464	11	65	71	59	9	93	54.5	21
MKS32	1.9	4.5	3.2	1.1	1.3	524	79	49	38	425	19	589	6	91	80	21	5	125	40	29
MKS51	1.8	4.1	2.5	1.1	1.7	410	153	55	87	354	22	561	29	349	71	30	7	107	35	29
Mean	2.1	5.0	2.4	1.3	1.7	406	108	60	53	592	22	757	13	126	84	30	6	151	47	37
Min	1.1	2.7	1.1	0.4	1.1	168	43	17	18	311	10	464	6	41	71	5	1	78	36	21
Max	4.6	9.3	3.4	3.2	2.3	717	155	143	87	1400	48	1140	29	349	104	59	9	350	62	74

These soils contain accepted 'background ranges' for As, Ba, Pb, Mn, Ni, V, and Zn according to the ANZECC soil investigation guidelines (Appendix 8). However, Cu in MKS13 (143 ppm) is above the background range (2-100 ppm) and indicates natural mineralisation in background areas.

2.5.2 Open pit soil

The pit 'soils', defined as the loose substrate on bench floors, have a maximum depth of 10 cm and are limited in thickness by the presence of continuous hard rock. Soils in the pit are the result of mining activity and represent finely crushed rock.

The soils (MKS1, MKS4, MKS5) in and around the open pit are weakly acidic (pH 6.1-7.0) to neutral. Soil conductivity is low (0 - 125 μS/cm). Open pit soils were sampled from; sulphide zones (MKS1 and MKS2), area of noticeable erosion (MKS3), and sites with elevated radioactivity (MKS6 and MKS16). Table 2.5 lists the geochemistry of pit soils.

Table 2.5. Major (wt%) and trace element (ppm) open pit soil geochemistry.

	Ca	Fe	K	Mg	Na	As	Ba	Ce	Cu	La	Mn	Ni	P	Pb	S	Sr	Th	U	V	Y	Zn
	%					ppm															
MKS1	12.4	12.8	0.4	0.1	0.4	33	97	683	1490	405	2810	203	1090	37	736	33	33	25	111	53	91
MKS2	7.1	12.0	0.6	1.6	0.9	21	97	388	1560	236	1890	277	684	11	1090	52	14	18	179	31	40
MKS3	8.3	21.0	0.8	0.3	0.6	97	156	311	4060	259	1320	162	1350	23	25610	25	20	20	108	43	25
MKS4	9.5	6.8	2.2	3.5	1.0	23	476	225	99	135	1670	82	562	6	339	150	12	12	193	29	32
MKS5	1.4	3.5	4.0	1.1	1.4	29	977	131	340	79	228	48	452	11	280	62	20	5	104	29	19
MKS6	7.4	8.2	2.2	1.4	0.8	36	409	1830	683	1110	1880	207	1520	43	2290	59	51	265	121	42	68
MKS16	4.7	6.0	1.8	1.9	1.3	21	335	652	316	434	1150	67	928	34	1050	59	29	45	135	36	75

Extreme values of Fe, S and Ce (max = Fe 21 wt%, S 2.6 wt%, Ce 0.2 wt%) as well as elevated mean contents of Mn (1564 ppm) and Cu (1221 ppm) were measured. The enrichment of pit soils over background by several orders of magnitude is due to its origin being finely crushed variably mineralised wall rock material.

Using log-normalised data, there are strong correlations (Appendix 4) between Fe, Mn, Cu, and S (r values Fe-Mn 0.7, Fe-Cu 0.81, Fe-S 0.77). Correlations are consistent with pit wall mineralogy (i.e. chalcopyrite, pyrite). Table 2.6 compares the average pit wall and average pit soil element geochemistry.

Table 2.6 Average pit wall (n=7) and average pit soil (n=7) major (wt%) and trace element (ppm) geochemistry.

	Ca	Fe	K	Mg	Na
	%				
MKPW	17	11	0.4	1	0.6
MKS	7	10	2	1	1

	As	Ba	Ce	Cu	La	Mn	Ni	P	Pb	S	Sr	Th	U	V	Y	Zn
	ppm															
MKPW	104	61	6973	1973	4743	2544	123	3082	169	11309	9	175	544	109	58	15
MKS	37	364	603	1221	380	1564	149	941	24	4485	63	26	56	136	38	50

2.6 Vegetation

Nineteen vegetation samples were taken from pit benches 944, 1000, 1048, 1080 and the main haul road. Metal concentrations of the ashed vegetation samples with corresponding soil locations are listed in Table 2.7.

Table 2.7. Major (wt%) and trace element (ppm) geochemistry of ashed *Aerva javanica, Acacia chisholmii, Asclepiadaceae Calotropis procera, Enneapogon lindleyanus, Aristida longicollis and Cymbopogon bombycinus* sampled from the open pit.

Sample	Ca	Fe	K	Mg	Na	As	Ba	Ce	Cu	La	Mn	Ni	P	Pb	S	Sr	Th	U	V	Y	Zn	Soil*
Aerva javanica (kapok bush)																						
MKV5	20.6	3.1	3.6	4.2	0.4	17	254	347	786	236	1760	247	15200	15	16300	270	11	10	28	13	410	MKS1
MKV6	21.9	2.4	2.4	5.2	0.2	19	81	216	477	164	327	117	7700	12	20010	272	6	7	22	7	177	MKS2
MKV13	19.8	0.9	2.6	6.4	0.2	8	650	30	90	20	570	24	10400	5	9450	323	2	3	26	4	47	MKS4
MKV14	20.2	2.9	1.9	3.8	0.5	16	14	737	208	497	540	42	5640	34	15300	147	15	153	27	10	54	Pitwall
MKV21	23.1	1.0	2.2	5.1	0.1	14	34	436	285	300	905	186	9690	12	11700	201	8	151	14	9	728	MKS6
MKV42	18.8	2.3	1.5	4.0	0.7	11	239	366	181	245	740	34	6720	22	14410	313	15	71	58	18	311	MKS16
Acacia chisholmii (Mineritchie Wattle)																						
MKV17	20.0	0.5	2.9	5.1	0.3	16	74	33	198	22	363	21	27900	10	21310	225	2	5	13	3	422	Road
MKV49	17.8	0.3	4.3	2.8	0.3	8	25	29	131	23	438	33	11900	5	25510	145	1	15	<10	2	721	MKS16
Calotropis procera																						
MKV11	13.3	0.1	4.9	6.9	0.2	5	38	6	60	6	2010	29	12700	5	59400	121	<1	<1	<10	1	111	MKS4
Enneapogon lindleyanus																						
MKV2	5.6	4.6	1.9	0.6	0.3	16	87	221	605	141	1260	265	2810	17	7170	48	10	8	42	15	193	MKS1
MKV46	4.0	1.2	1.3	0.9	0.4	8	75	266	80	184	446	50	2050	11	8090	36	7	22	30	8	168	MKS16
Aristida longicollis																						
MKV4	2.0	1.4	1.6	0.3	0.1	7	106	87	246	55	843	43	1900	5	3510	31	4	3	13	5	222	MKS1
MKV22	3.0	1.0	2.5	0.9	0.2	7	44	250	158	162	376	41	2830	9	12100	44	6	69	19	5	474	MKS6
MKV47	3.0	0.7	1.6	0.8	0.2	5	70	89	68	60	461	30	2890	7	12800	57	4	13	20	5	305	MKS16
MKV12	2.6	0.9	1.6	1.0	0.1	5	120	29	40	19	555	35	3570	6	1030	58	1	3	23	3	78	MKS4
Cymbopogon bombycinus																						
MKV3	5.7	2.9	1.8	1.3	0.2	10	98	159	525	94	1770	97	7920	16	12210	53	10	7	27	10	706	MKS1
MKV10	4.9	1.1	1.9	1.3	0.2	7	79	38	56	24	884	70	6230	5	2190	65	2	2	27	5	354	MKS4
MKV20	5.0	2.5	1.7	1.7	0.2	23	36	782	571	554	1110	146	2410	26	28710	30	16	318	25	10	660	MKS6
MKV48	4.7	2.9	3.4	1.2	1.0	12	232	445	153	302	968	37	1620	16	7060	61	16	33	70	22	466	MKS16

*Corresponding soil sample location.

Vegetation samples MKV20, MKV21 and MKV22 were collected on a substrate (MKS6) with a high radioactivity (21.9 mSv/yr). At this site, the highest concentrations of Cu (571 ppm), Mn (1110 ppm), Ce (782 ppm), La (554 ppm) and U (318 ppm) occur in *Cymbopogon bombycinus* (MKV20).

Aerva javanica (kapok bush) has strong positive correlations between (log_{10} n=6) Cu and Ni (r=0.85), Zn and Ni (r=0.79), Ce with La-Pb-U (r>0.8) and a strong negative correlation between Th and Mg (r=-0.98). *Cymbopogon bombycinus* (Silky Oilgrass) has strong positive correlation values of (log_{10} n=4) Cu-Zn (r=0.97), Cu-S (0.85), Zn-Mn (r=0.80), Ni-Mg (r=0.94) and high correlation of S with U-REE (r>0.9).

Figure 2.5. Cumulative bar graph displaying the geochemistry of *Aerva javanica*.

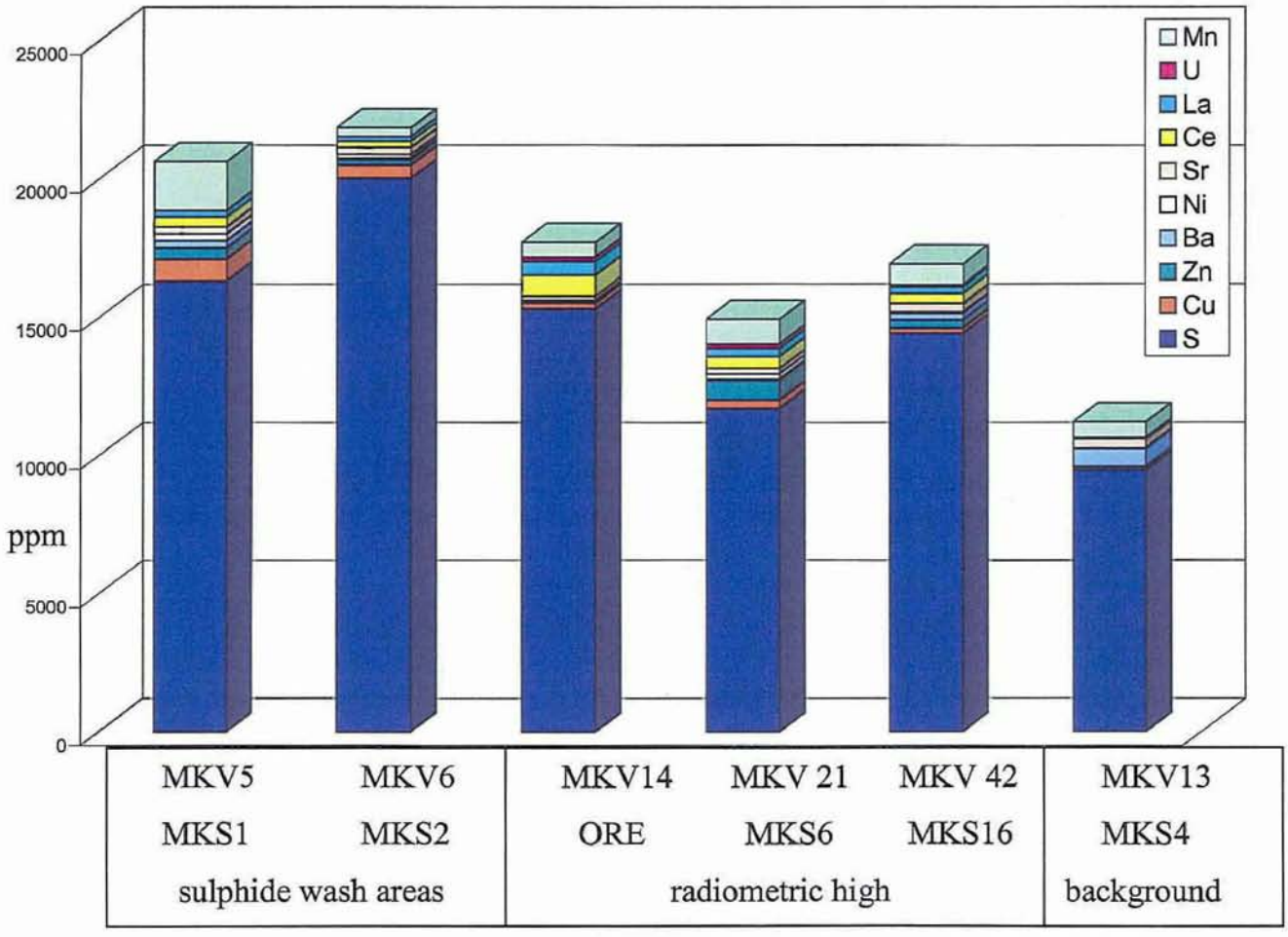

Figure 2.6a. Bar graph illustrating the plant soil ratio of *Aerva javanica*.

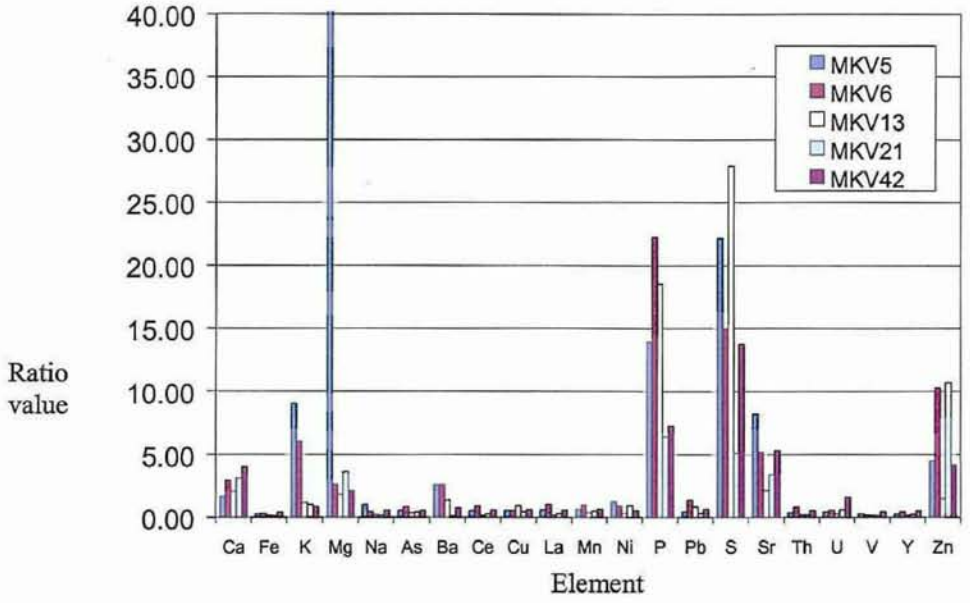

Figure 2.6b. Bar graph illustrating the plant soil ratio of *Enneapogon lindleyanus*

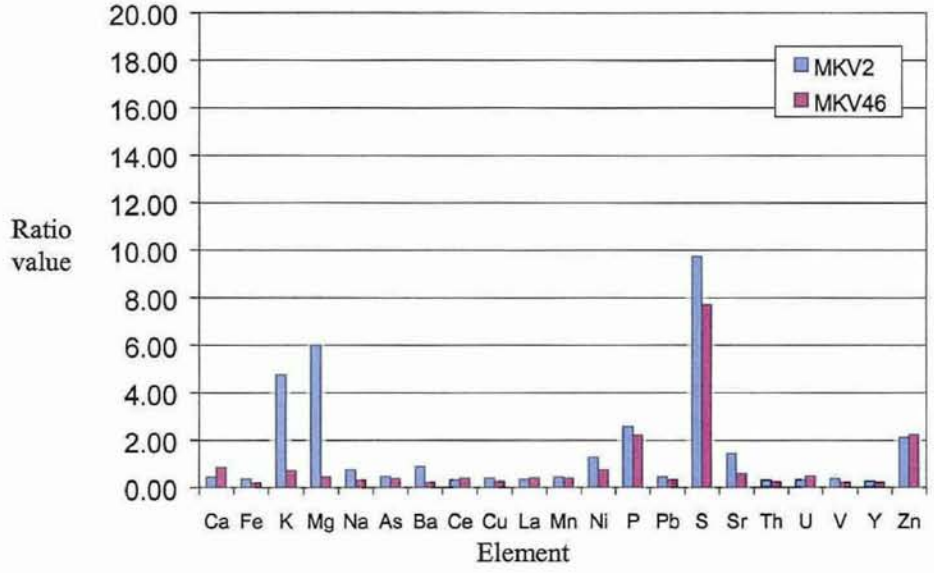

Figure 2.6c. Bar graph illustrating the plant soil ratio of *Aristida longicollis*.

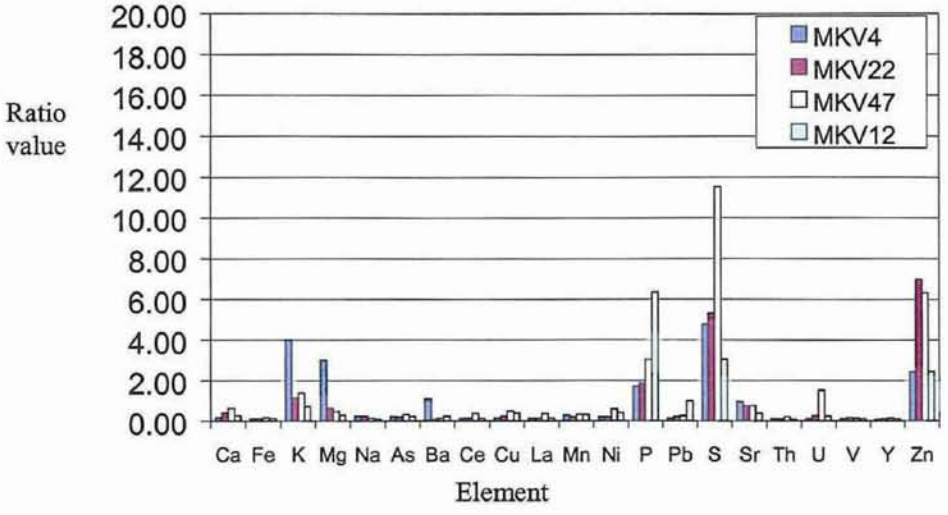

Figure 2.6d. Bar graph illustrating the plant soil ratio of *Cymbopogon bombycinus*

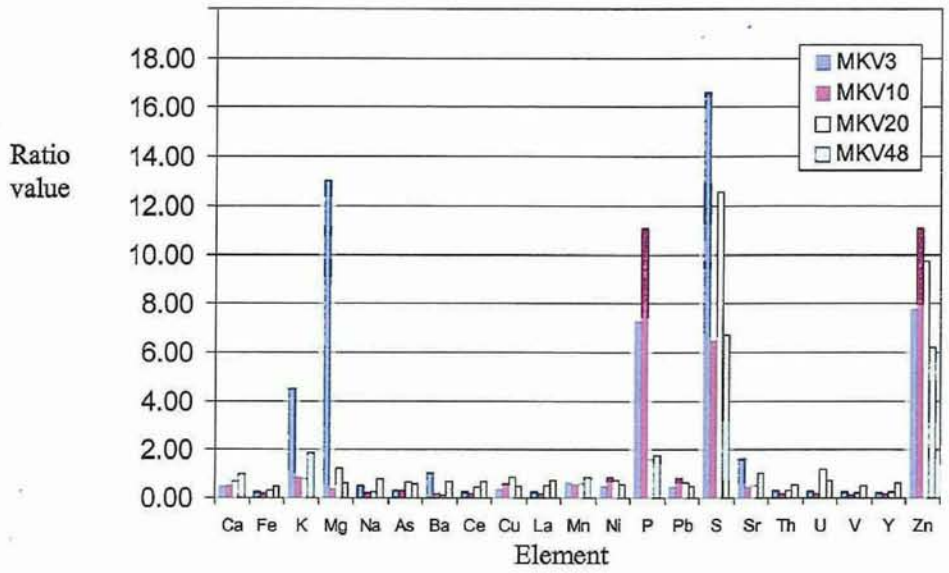

Plant ash to soil ratios (Appendix 4) for Ca, K, Mg, Ba, P, S, Sr and Zn are high in the plants sampled in the open pit (Figure 2.6a-d). As dry weight values are not available discussion of biaccumulation estimates in regard to specific elements in these plants is speculative, as there is preferential accumulation from dry plants into ashed plants. It is clear however, elemental concentrations in ashed plant material reflects elemental soil concentrations (eg availability of uranium).

Soils in the open pit are derived from past mining activities and active erosion of the pit walls and floors. Physical weathering of pit wall material is occurring and the erosion of particles disperses U, Cu, S etc into the pit with seasonal rain. Pit soils exceed ANZECC (1992) environmental soil quality guidelines for Cu (1200ppm) and Ni (130ppm) which are set at 60 ppm for Cu and Ni for environmental investigation. Limited nutrient concentrations appear to be available (P 941 ppm). However, lack of soil structure and poor water retention capabilities do not encourage vegetation.

2.7 Water

The open pit lake is approximately 40 m deep and holds approximately 54 million litres of water (depending on seasonal variation). The water was a vivid blue colour with efflorescences evident at the edge of the water. No fauna was observed. The spring at

RL944 contained filamentous green algae and drained into the pit. Water samples were collected from Corella Dam (MKW1 at 400770E, 7695446N), the open pit (MKW2) and from level 944 the spring/wetland zone (MKW3). Table 2.8 lists the major ionic composition and trace metal analyses from Corella Dam (background) and open pit water samples.

Table 2.8. Water chemistry (MKW1 Corella dam, MKW2 pit lake, MKW3 pit spring).

Parameter	MKW1	MKW2	MKW3
Major Ionic Composition			
pH	8.38	6.11	7.6
Conductivity (µS/cm)	206	5050	3420
Total Hardness (mg $CaCO_3$/L)	70.9	1735	1390
Total Alkalinity (mg $CaCO_3$/L)	810	2.5	335
Total Dissolved Solids (mg/L)	105	2720	1910
Sodium (mg/L)	12.4	152	900
Potassium (mg/L)	4.6	8.3	7.9
Calcium (mg/L)	21.3	464	350
Magnesium (mg/L)	4.3	140	126
Sulphate (mg/L)	9.1	1840	1100
Chloride (mg/L)	4.9	109	41.3
Bicarbonate (mg/L)	98.8	30	408
Copper (µg/L)	<0.5	1170	20
Iron (µg/L)	120	3230	2610
Manganese (µg/L)	<1	1050	32
Molybdenum (µg/L)	<1	2	12
Nickel (µg/L)	<0.2	688	31
Lead (µg/L)	<1	<1	<1
Antimony (µg/L)	<0.1	<0.1	<0.1
Uranium (µg/L)	1	460	398
Zinc (µg/L)	<10	88	17
Dissolved Oxygen (mg/L)	6.77	6.8	2.65

Open pit waters have high conductivity, TDS, Ca, SO_4, Cl and metal concentrations (Cu, Fe, Mg, U and Zn) compared to background and spring water. Dissolved oxygen in the open pit is at 6.8 mg/L and lowest in the seepage waters at 2.65 mg/L. Plotting water analyses on a Piper diagram (Figure 2.7) illustrates that open pit waters are relatively enriched in Ca, Mg, SO_4, and Cl compared to background waters, which have higher HCO_3^- values.

Figure 2.7. Piper diagram illustrating the chemistry of open pit and Corella Dam waters.

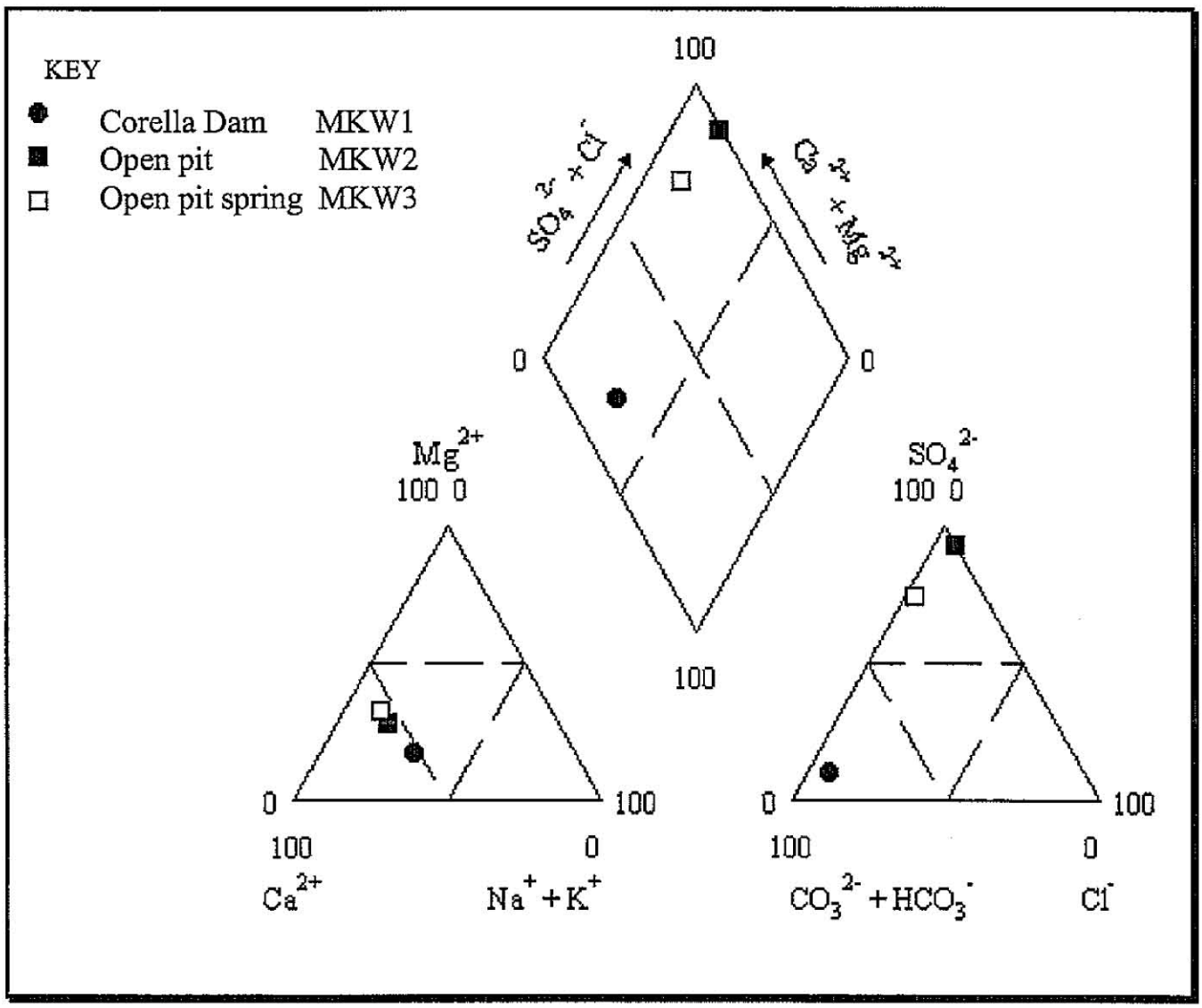

2.8 Radiometric survey

2.8.1 Radiometric survey design

The open pit ground gamma-ray survey was designed to establish dose rates and known and unknown radiation sources. The survey was conducted on foot and followed pit benches and the main haul road and crossed the waste rock pile. Radiometric readings were taken from point to point continuously (Appendix 1). Exposure rates for environmental data (μR/hr, nSv/hr) and assays for geophysical data (cps; equivalent concentrations of %K and ppm U and Th) were recorded. All radiometric data were tabulated and assessed for data quality. Exposure rates were converted from nSv/hr to mSv/year. Ratios for %K/ppmTh, ppmU/ppmTh and %K/ppmU were calculated. Total count was recorded using a Scintrex- BGS-1SL scintillometer, the traverses were surveyed at a speed of approximately 0.16 m/s and a height of 1m over dry ground.

2.8.2 Geophysical analysis

The measured dose rate for the completed survey range from 0.96 mSv/year to 25.4 mSv/year (average 5.6 mSv/year, n=72). Traverses RL960, RL1000 and RL1048 along the eastern face (Figure 2.9a) have the highest dose rates (26 mSv/yr). The waste rock pile at the base of the pit has a moderate does reading of 10.7 mSv/yr. Traverses along the western face (Figure 2.9b) have low dose at background levels (<2mSv/yr).

Total count (TC) readings are highest along RL960 at the NE to SE pit face (Figure 2.10). A total count anomaly (1500 cps) is present in the waste rock pile area. Thorium and uranium signatures follow total count rates. The potassium signature also conforms to the total count signature with the exception of two areas. At 397240E 7705500N and 396900E 7705350N, %K increases when Th, U and TC traces decrease, possibly due to a change in rock type.

Maximum U (ppm) readings correspond to the eastern face (Figure 2.11) exposed ore lenses and the waste rock pile at the base of the pit. At radiometric survey points where uranium concentrations exceeded 150 ppm, accurate readings were not recorded as GR-320 spectrometer specifications do not allow for such high concentrations.

Figure 2.9. Exposure rate (mSv/year) of RL960, RL1000, RL1048 along the eastern pit wall.

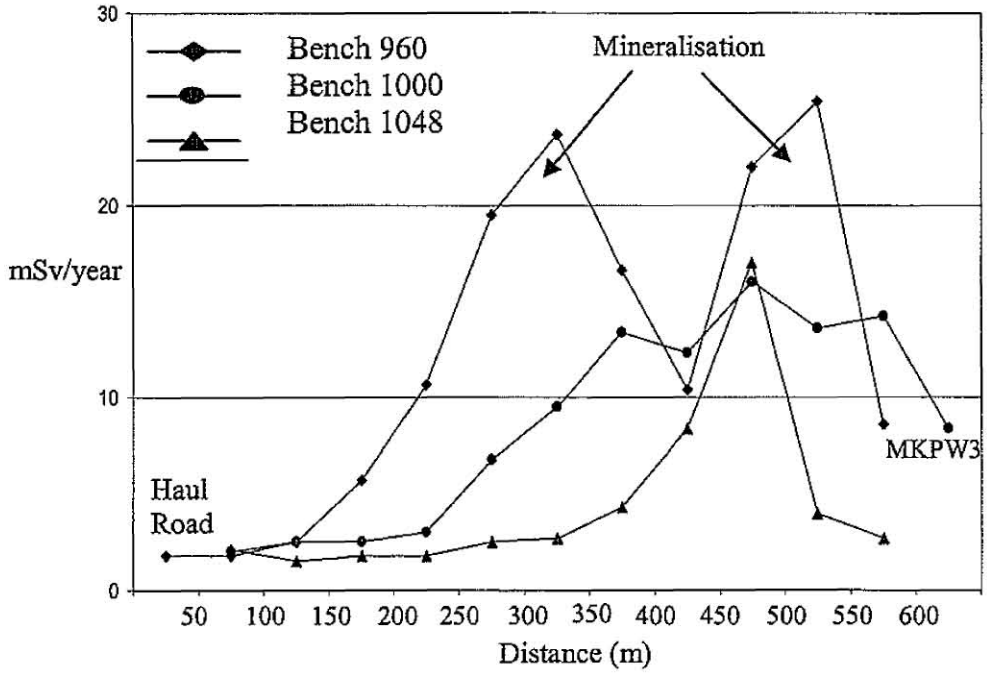

Figure 2.9b. Open pit exposure rate (mSv/year)

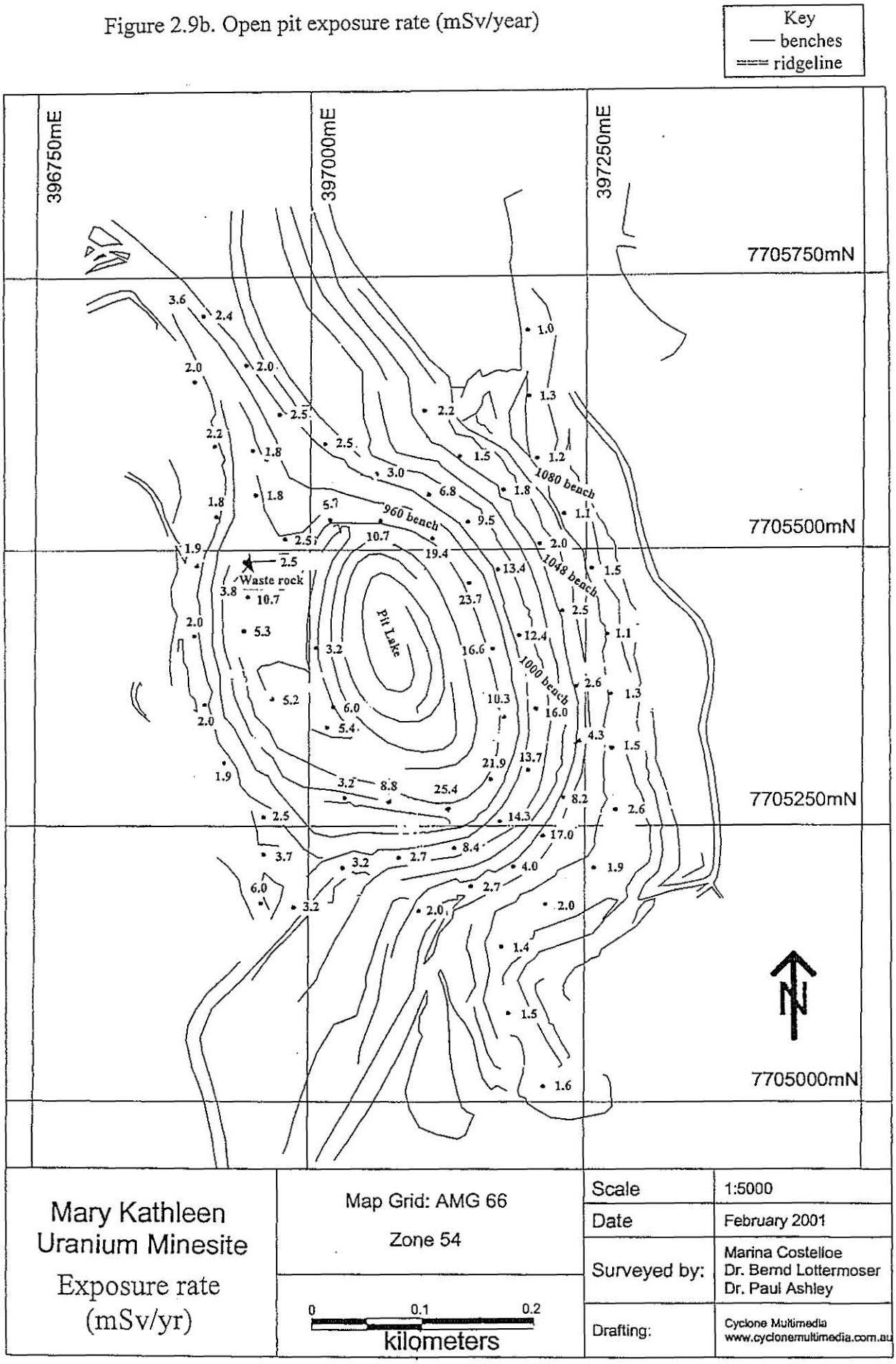

Figure 2.10 Open pit total count map (cps).

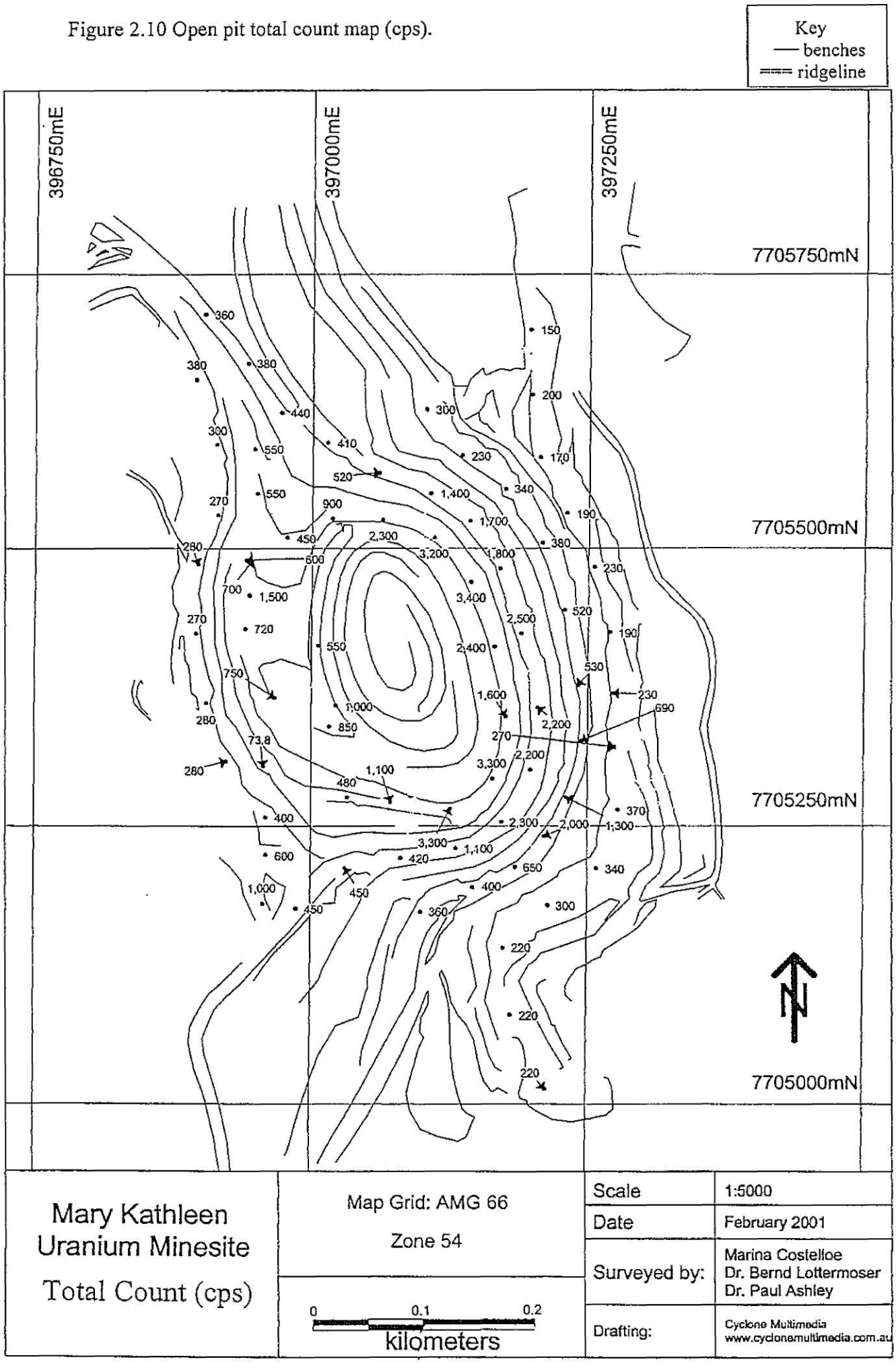

Figure 2.11. Open pit uranium map (ppm)

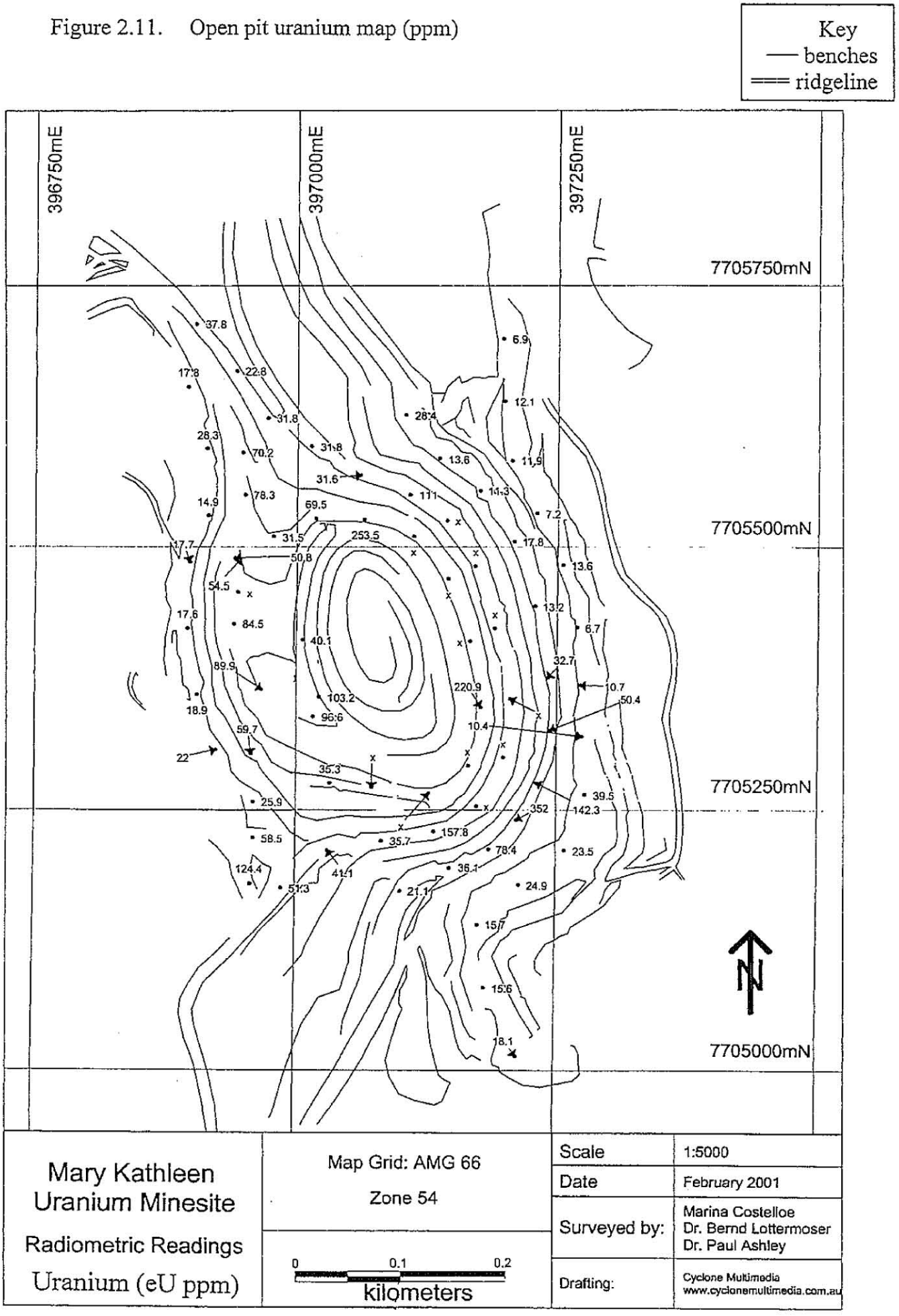

2.9 Discussion

2.9.1 Mineral efflorescence formation and dissolution

Open pit mineralogy, for example, grossular $Ca_3Al_2(SiO_4)_3$, clinopyroxene (diopside) $CaMg(Si_2O_6)$, allanite $(Ca,Ce,La)_2(Al,Fe)_3(SiO_4)_3(OH)$, chlorite $(Mg,Fe)_5Al(AlSi_3)O_{10}(OH)_9$, calcite pyrrhotite ($Fe^{2+}{}_{0.95}S$), chalcopyrite ($CuFeS_2$), pyrite ($FeS_2$), marcasite ($FeS_2$), galena (PbS), sphalerite ((Zn,Fe)S) and uraninite (UO_2) dictates the availability of elements (Ca, Ce, Cu, Fe, La, Mg, U etc.) contributing to mineral efflorescences.

Surficial oxidation of ore and adjacent sulphide-bearing calc-silicate rocks has led to contemporary precipitation of mineral efflorescences on the pit walls. Oxidation of pyrite may be considered to take place in three major steps: (1) oxidation of pyrite to generate ferrous iron; (2) oxidation of ferrous iron to ferric iron; and (3) oxidation of pyrite by ferric iron (Nordstrom, 1979, 1982; Sato, 1992; Jambor, 1994; Bigham, 1994; Bigham et al., 1996; Schwertmann et al., 1995; Kesler, 1997; Nordstrom and Alpers, 1999):

$$(1)\ FeS_2 + 7/2\ O_2 + H_2O \rightarrow Fe^{3+} + 2\ SO_4^{2-} + 2\ H^+$$

$$(2)\ Fe^{2+} + \tfrac{1}{4}\ O_2 + H^+ \longrightarrow Fe^{3+} + \tfrac{1}{2}\ H_2O$$

$$(3)\ FeS_2 + 14\ Fe^{3+} + 8\ H_2O \longrightarrow Fe^{2+} + 2\ SO_4^{2-} + 16\ H^+$$

Wallrock oxidation of reactive sulphides produces metal rich, acidic (sulphuric H_2SO_4) solutions (Plumlee, 1999). A reaction likely to occur during flushing is the dissolution of melanterite (Fernandes et al., 1998):

$$Fe(SO_4).7H_2O + 1/4O_2 \longleftrightarrow Fe(OH)_3 + H_2SO_4 + 4.5H_2O$$

Water soluble sulphates (i.e. melanterite, chalcanthite) formed under oxidizing conditions and high evaporation rates, can release significant amounts of metals and acid upon redissolution (Plumlee et al. 1999). This is an important factor leading to seasonal fluctuations in contamination levels of ground and surface waters, especially in semi-arid and arid climates (Alpers et al., 1994; Dold et al., 1999). At Mary Kathleen, pit geometry promotes runoff from the catchment and remobilises deposited metals (i.e. Cu, Mn, U, Ce, La) into the pit lake via the dissolution of these soluble efflorescence salts influencing the chemical composition of the pit lake.

Thiobacillus ferooxidans is an iron oxidising bacteria that oxidises sulphide minerals (pyrite, chalcopyrite, sphalerite, arsenopyrite and pyrrhotite) to form ferric sulphate and sulphuric acid.

$$4\ FeS_2 + 15O_2 + 2H_2O \rightarrow 2\ Fe_2(SO_4)_3 + 2H_2SO_4$$

Also 'bioleaching' can mobilise uranium from adjacent sulphide minerals also. Ferric iron is an oxidant for U^{4+} and therefore the dissolution of uranium oxides can be represented with these two reactions represented by the following equations (Bruynesteyn and Hackl 1990)

$$UO_2\ (s) + 2\ Fe_2(SO_4)_3 + 2H_2SO_4 \rightarrow UO_2(SO4)_3^{4-} + 2FeSO_4 + 4H^+$$

$$UO_3 + (s) + 3\ H_2SO_4 \rightarrow UO_2(SO4)_3^{4-} + H^+ + H_2O$$

2.9.2 Plant growth and bioaccumulation processes

Geochemical analyses of ashed vegetation indicate that *Acacia chisholmii* (wattle), *Aerva javanica* (kapok bush), *Triodia longiceps* (porcupine spinifex) and other species of grass are tolerant to high levels of U (max 318 ppm) and other metal contaminants (max; Ni 247 ppm, Mn 2010 ppm, Ce 782 ppm, La 554 ppm). Plant concentration ratios are found to vary with the concentration of the contaminant in soil, especially for S, Sr and Zn.

The ratio of plant ash values on contaminated versus background sites show high levels of metals including Ce, La, Mn, U and Zn indicating the dispersal of these elements into the ecosystem. The highest plant to soil ratio for plants within the open pit include K, Mg, P, S and Zn.

Neutralisation of acids (generated by the dissolution of mineral efflorescences) by carbonates create a near neutral soil pH which assists plant growth. Dry weather conditions and thin substrate material are the main constrains for vegetation growth within the open pit.

2.9.3 Final void water quality.

Hydrologic flow in the pit is governed by wall rock characteristics and pit wall fractures. Seasonal precipitation and seasonal run off flows down pit walls into the pit lake. Pit waters are also affected by groundwater flow from the seepage area and by evaporation. A small and constant bicarbonate discharge emanates from the seepage area (RL944). Hence, the pit lake's pH is only slightly acidic (pH 6.1).

Water soluble sulphates react with acid-neutralising minerals such as carbonates. Calcite is abundant in the open pit and its reaction

$$CaCO_3 + H^+ \rightarrow Ca^{2+} + HCO_3^-$$

buffers at near neutral pH (6.5 - 7). HCO_3^- is therefore the principal species influencing the water pH (Al et al., 1994; Dold et al., 1999). Buffering reactions of pit rock sulphides with gangue calc-silicates and carbonate phases are preventing low pH conditions from developing. Similar pH-buffering reactions have been studied in other geological settings (Nordstrom and Munoz, 1986; Dubrovsky et.al., 1984; Plumlee, 1999).

The Mary Kathleen pit lake contains high levels of sulphate and dissolved metals (Cu, Fe, Mn, Ni and U). Metal concentrations of Cu, and U exceed the recommended water quality guideline values (low risk) for heavy metals in livestock drinking water (ANZECC, 2000). Uranium concentration is double the livestock drinking value of 200 µg/L and is twenty times greater than the guideline of 20 µg/L for drinking water (ANZECC, 2000). Hardness, total dissolved solids (TDS), Mn, Ni and SO_4 exceed the health considerations in the guidelines for drinking water (NH&MRC 1996). The hardness-modified trigger value for 80% Level of Protection in MKW2 was exceeded for Cu and Ni (Appendix 8).

Assuming that the calculated radiological value of uranium in the pit lake for 300µg/L U is equivalent to approximately 3.8 Bq/L (NH&MRC 1996), the safety limit of 0.5 Bq/L (NH&MRC 1996) is exceeded. Other radionuclides (i.e. Th, Ra, K nuclides) may also be present and increase the above mentioned calculated radiological value further.

2.9.4 Radioactivity and exposure assessment

Gamma radiation is detected to a maximum source depth of 50 cm (Grasty and Darnley, 1971). Shallow soils (approx.10 cm) exist within the open pit, hence signals were most representative of parent materials.

Exposure rates were highest at the base of the pit where the pit geometry exposes thicker ore seams. Measured exposure rates (with the exception of three sites on RL960) were at or below 20 mSv/yr. The Australian Radiation Protection Standards stipulate a maximum safe limit, termed 'occupational exposure', at 20 mSv/yr averaged over five consecutive years (NH&MRC, 1995). The global background for the individual dose of radiation from natural sources has been estimated to be 2.4 mSv/yr (UNSCEAR, 2000). Australian data suggest that the average annual dose in this country may be slightly lower at approximately 2 mSv/yr (Webb et al., 1999). Average exposure rate in the pit was 5.6 mSv/year. Significantly lower exposure rates were recorded away from the eastern wall (2.4 mSv/yr, n=40) and are close to global background levels.

2.9.5 Final void management

Open pit geochemical processes and water quality preclude the use of the Mary Kathleen void as a water storage facility, wetland/wildlife habitat or aquaculture pond development. The open pit would not provide a viable waste repository site due to potential ground water contamination (D.I.S.R., 1999). An engineered solar pond to generate electricity and desalinate or distil water, has limited potential due to the cost of development and the distance to end users.

Various factors including community needs, costs, government policy and location determines the management and possible end-use options for open pits. Development into a heritage site is the most suitable management option for the open pit at Mary Kathleen. Considering the area's aesthetic qualities and historical significance the site lends itself to tourist development. Public access to the lake water should be restricted and notification of its water quality clearly signposted. Radiation exposure can be reduced to normal background levels by blocking access to high dose areas. Visitor access should be confined to a clearly marked sign posted walkway. These precautions will enable the area to be managed as a heritage park.

2.10 Summary

The open pit geochemistry is defined by elevated uranium concentration and significant REE levels, as well as high Ca, Fe and S concentrations contained in the amphibolite grade metamorphosed calc-silicate, mafic to intermediate igneous and sedimentary host rocks. Water soluble sulphates such as melanterite, copiapite and chalcanthite form under oxidising conditions and high evaporation rates on pit walls. During the wet season, the dissolution of these salts can remobilise metals (e.g. Fe, Ce, Cu, Mg and U) into the pit lake. The mobilisation of these salts impacts on the water quality of the pit lake.

Background soils are generally considered to be within background ranges (ANZECC 2000) with the exception of one Cu value. Open pit soils have extreme values of Fe, S, Ce, Cu and Mn compared to background samples. Shallow pit soils, being derived from pit wall material have similar mineralogies and geochemistry.

Vegetation within the open pit bioaccumulate high levels of metals including Ce, La, Mn, U and Zn indicating the dispersal of these elements into the ecosystem. The highest plant to soil ratio for plants within the open pit include K, Mg, P, S and Zn.

Concentrations of U, Mn, Ni and Cu within the open pit lake exceed water safety limits for domestic, industrial, recreational and agricultural use (ANZECC 1992, ANZECC 2000). Uranium (460 μg/L or approx 3.8 Bq/L) in particular is considered excessive both in chemical and radiological guidelines and requires monitoring. Further water quality monitoring is required. Public access to the lake water should be deterred and notification of the water quality clearly signposted.

Open pit radiation levels exceed 20 mSv/yr on the south eastern pit face, clearly measuring radiation emitted from ore lenses. A discrete high was also measured over the waste rock pile at the base of the pit. Background levels of less than <2.4 mSv/yr were measured on the west pit faces.